Check for updates

Received: 12 January 2022 | Revised: 22 December 2022 | Accepted: 13 January 2023

DOI: 10.1002/mma.9125

RESEARCH ARTICLE

WILEY

An ETD method for multi-asset American option pricing under jump-diffusion model

Rafael Company[1] | **Vera N. Egorova**[2] | **Lucas Jódar**[1]

[1]Instituto de Matemática Multidisciplinar, Universitat Politécnica de Valéncia, Valencia, Spain

[2]Departamento de Matemática Aplicada y Ciencias de la Computación, Universidad de Cantabria, Santander, Spain

Correspondence
Vera N. Egorova, Departamento de Matemática Aplicada y Ciencias de la Computación, Universidad de Cantabria, Avenida de los Castros, s/n, 39005 Santander, Spain.
Email: vera.egorova@unican.es

Communicated by: M. Rasmussen

Funding information
Ministerio de Ciencia, Innovación y Universidades, Grant/Award Number: MTM2017- 89664-P; Ministerio de Economía y Competitividad, Grant/Award Number: PID2019-107685RB-I00

In this paper, we propose a numerical method for American multi-asset options under jump-diffusion model based on the combination of the exponential time differencing (ETD) technique for the differential operator and Gauss–Hermite quadrature for the integral term. In order to simplify the computational stencil and improve characteristics of the ETD-scheme mixed derivative eliminating transformation is applied. The results are compared with recently proposed methods.

KEYWORDS

exponential time differencing, jump-diffusion model, multi-asset option pricing, multivariate Gauss-Hermite quadrature, partial-integro differential equation

MSC CLASSIFICATION

35R35, 65M06, 65M22

1 | INTRODUCTION

The class of multi-asset option pricing problems have an increasing interest among the practitioners because they are frequent in the real market practice. The price of such multi-asset options can be found by the well-known Black–Scholes model [1]. Despite its simplicity and elegance, it does not take into consideration the possibility of the abrupt variations in the stock prices, which emerges a suitable generalization of the Black–Scholes model. In particular, jump-diffusion models assume that underlying assets price process presents jumps at random times due to some force majeure events. In that case, from the mathematical point of view, the partial differential problem of option pricing becomes a partial integro-differential equation (PIDE) [2], where the integral part is non-local. In addition, for multi-asset problems the nature of this integral term is multiple [3], which adds more complexity.

The flexibility of American options to be exercised at any moment before the maturity leads to a very challenging free boundary PIDE problem. One of the most used methods for treating the American option pricing problem is the penalty method that incorporates an additional term to the original equation for European case [4], resulting in a semi-linear PIDE for the jump-diffusion problem. Since the closed-form solution does not exist, some numerical approximation is required.

The resulting PIDE with the possibility of the early exercise has been studied by various authors. Bensoussan and Lions [5] characterized price of a put option in terms of a solution of a system of partial-integro differential inequalities (see also [6]). Wang et al. [7, 8] investigated a penalty method for solving a linear complementarity problem using a power penalty

This is an open access article under the terms of the Creative Commons Attribution-NonCommercial License, which permits use, distribution and reproduction in any medium, provided the original work is properly cited and is not used for commercial purposes.
© 2023 The Authors. Mathematical Methods in the Applied Sciences published by John Wiley & Sons, Ltd.

term for the case without jumps in the underlying asset dynamics. Lesmana and Wang [9] proposed a power penalty method for solving the free boundary problem for pricing American options under transaction costs. Penalty methods for American option pricing under stochastic volatility models are studied in the paper Zvan et al. [4] d'Halluin et al. [10] investigated a penalty method for American options on jump-diffusion underlying processes. In Cruz and Ševčovič [11], the variational inequality was rigorously derived under additional condition $\int_0^\infty (e^y - 1)g(y)dy \leq r$ relating the Levy measure $\nu(dy) = g(y)dy$ and the interest rate r.

For multidimensional problems, one of the most used techniques is the semi-discretization. The spatial derivatives are approximated by finite differences (FD) [12–16] or finite element method [17, 18]. Some methods are based on the radial basis function (RBF) approximation for the spatial derivatives [19]. Usually, the time-stepping is performed by the standard Crank–Nicolson scheme or backward difference. In Shirzadi et al. [20], the mesh-free method based on moving least squares collocation is considered. However, in the cited above papers, the problems are limited to one or two assets in the portfolio. This important lack motivates us to consider more general n-dimensional problem.

Another important numerical challenge is related to the correlated assets. The presence of the mixed derivative terms in the PIDE is the source of many computational drawbacks and may cause instabilities and inaccuracies. The negative effect of the mixed derivative terms increases exponentially with the growth of the dimensionality of the problem. Thus, it is extremely important to address this issue in multi-dimensional cases. In present paper, we use the approach based on LDL^T-factorization of the so-called diffusion matrix [21]. This mixed derivative removing technique allows avoiding of the numerical drawbacks and reducing significantly the computational cost.

There are a variety of multi-asset options, which differ to each other by the payoff function. This payoff function defines the initial and boundary conditions. The considered mixed derivative removing algorithm transforms the original semi-infinite domain to an infinite one. For the numerical solution, it is truncated, thus at the boundaries of this new truncated domain the PIDE is valid and can be used as the boundary conditions. This makes the proposed algorithm more versatile and flexible to an option type.

Since the jump-diffusion model is considered, the corresponding non-local integral term has to be handled. In Boen and Hout [3], as well as in many other papers cited above the trapezoidal rule is employed. However, it requires additional computational resources and leads to a dense matrix discretization [19] for FD methods. This drawback can be avoided by applying the fast Fourier transform [22]. Moreover, the integration domain is infinite and thus has to be truncated, which affects to the accuracy. An alternative approach for numerical approximation of improper integrals is the Gauss–Hermite quadrature, which allows an accurate approximation of the improper integral with a very low number of quadrature nodes. Since the nodes not necessary coincide with the mesh points of the computational domain of the spatial discretization, an interpolation is to be employed. In Fakharany and Egorova [14], the bi-variate Gauss–Hermite quadrature is applied to the two-asset option under the jump-diffusion model. In present paper, we generalize it to n-dimensional case by proposing a multi-dimensional interpolation algorithm.

In present paper, we follow the semi-discretization approach, the second-order central FD scheme are used for the spatial derivatives approximation. The time-stepping is performed by the exponential time differencing (ETD) method [23] based on exact integration of the system of ordinary differential equations. This approach has been previously tested by authors on one-dimensional Heston model valuation [24] and jump-diffusion models [25].

The rest of paper is organized as follows. In Section 2, the PIDE is derived for the European and American option values under the multi-asset jump-diffusion model. Section 3 describes the mixed derivative removing algorithm in n-dimensional case. Section 4 proposes the numerical GH-ETD method for the transformed problem. This method includes: the discretization of the initial and boundary conditions, as well as the spatial differential operator; the multivariate Gauss–Hermite quadrature, which uses the multi-linear interpolation; and, finally, the ETD method. The results are presented and discussed in Section 5. In Section 6, some conclusions are drawn.

2 | JUMP-DIFFUSION MODEL FOR MULTI-ASSET OPTION

Let us consider a set of M assets $\mathbf{S} = (S_1, S_2, \dots, S_M)$ under jump-diffusion model for price dynamics which incorporates the stochastic volatility and Poisson jumps, such that for each $i = 1, \dots, M$ one has

10991476, 2023, 9, Downloaded from https://onlinelibrary.wiley.com/doi/10.1002/mma.9125 by Universidad De Cantabria, Wiley Online Library on [16/05/2023]. See the Terms and Conditions (https://onlinelibrary.wiley.com/terms-and-conditions) on Wiley Online Library for rules of use; OA articles are governed by the applicable Creative Commons License

$$\frac{dS_i(t)}{S_i(t)} = (r - q_i - \lambda\kappa_i)dt + \sigma_i dW_i + (e^{J_i} - 1)dZ(t),\ i = 1, \dots, M, \tag{1}$$

where r is the risk free interest rate, q_i and σ_i, $i = 1, \dots, M$, are dividend yields and asset volatilities, conditional on the event that no jumps occur, respectively; W_i, $i = 1, \dots, M$, stand for standard Brownian motions pairwise correlated by $\rho_{ij} \in (-1, 1)$, $i, j = 1, \dots, M$. We consider a model with jumps of the sizes J_i, κ_i represent the expected relative jump sizes ($\kappa_i = \mathbb{E}[e^{J_i} - 1]$), $Z(t)$ is a Poisson process with jump intensity λ and is independent of the standard Brownian motion [26].

2.1 | European options

Let us consider a multi-asset European-style option with maturity $T > 0$ written on the assets (1) and let its price be a function of the time to maturity $\tau = T - t$ and the asset values $\mathbf{S}$ denoted by $V(\mathbf{S}, \tau)$. Based on Ito calculus, the option value satisfies the following PIDE

$$\begin{aligned}\frac{\partial V}{\partial \tau} =& \frac{1}{2}\sum_{i,j=1}^{M} \rho_{ij}\sigma_i\sigma_j S_i S_j \frac{\partial^2 V}{\partial S_i \partial S_j} + \sum_{i=1}^{M}(r - q_i - \lambda k_i)S_i \frac{\partial V}{\partial S_i} - (r + \lambda)V \\ &+ \lambda \int_{\mathbb{R}_+^M} V(\mathbf{S}\cdot\mathbf{y}, \tau) f(\mathbf{y}) d\mathbf{y},\end{aligned} \tag{2}$$

where $\mathbb{R}_+^M = \left\{\mathbf{y} \in \mathbb{R}^M \,|\, y_i \geq 0, i = 1, \dots, M\right\}$; ρ_{ij} are the entries of the symmetric positive semi-definite correlation matrix

$$R = \left\{\rho_{ij}\right\}_{1 \leq i,j \leq M}, \tag{3}$$

such that $\rho_{ii} = 1$, $\rho_{ij} = \rho_{ji}$, $i \neq j$, and $|\rho_{ij}| \leq 1$. Function $f(\mathbf{y})$ is the probability density function of a multivariate lognormal distribution.

At the maturity $\tau = 0$, the option price is a payoff function:

$$V(\mathbf{S}, 0) = \varphi(\mathbf{S}), \tag{4}$$

which is defined by the contract type.

Note that the proposed here numerical algorithm is applicable to any type of multi-asset option as it will be explained later.

It is well-known that logarithm transformation for spatial variables leads to constant coefficient partial differential equation [22]. Thus, we apply the following dimensionless transformation:

$$x_i = \log\frac{S_i}{E}, \qquad 1 \leq i \leq M, \tag{5}$$

with $V(S, \tau) = EU(X, \tau)$, where $X = (x_1, x_2, \dots, x_M)^T$ and E is the strike price. Then, it results in the following PIDE:

$$U_\tau(X, \tau) = \mathcal{D}U(X, \tau) + \mathcal{I}U(X, \tau), \tag{6}$$

with differential operator

$$\mathcal{D}U = \frac{1}{2}\sum_{i,j=1}^{M} \rho_{ij}\frac{\partial^2 U}{\partial x_i \partial x_j} + \sum_{i=1}^{M}\left(r - q_i - \lambda\kappa_i - \frac{\sigma_i^2}{2}\right)\frac{\partial U}{\partial x_i} - (r + \lambda)U; \tag{7}$$

and integral operator $\mathcal{I}U$ is given by the following:

$$\mathcal{I}U(X, \tau) = \lambda \int_{\mathbb{R}^M} U(X + \boldsymbol{\eta}, \tau) g(\boldsymbol{\eta}) d\boldsymbol{\eta}, \tag{8}$$

10991476, 2023, 9, Downloaded from https://onlinelibrary.wiley.com/doi/10.1002/mma.9125 by Universidad De Cantabria, Wiley Online Library on [16/05/2023]. See the Terms and Conditions (https://onlinelibrary.wiley.com/terms-and-conditions) on Wiley Online Library for rules of use; OA articles are governed by the applicable Creative Commons License

where $\boldsymbol{\eta} = (\eta_1, \dots, \eta_M) \in \mathbb{R}^M$. The probability density function of the multivariate normal distribution $g(\boldsymbol{\eta})$ is defined as follows:

$$g(\boldsymbol{\eta}) = \frac{1}{(2\pi)^{M/2}\sqrt{|\Sigma|}} \exp\left[-\frac{1}{2}(\boldsymbol{\eta} - \mu)\Sigma^{-1}(\boldsymbol{\eta} - \mu)^T\right], \tag{9}$$

where $\mu = (\mu_1, \mu_2, \dots, \mu_M)$ are the means of the jumps, and Σ is the covariance matrix of the jumps [26],

$$\Sigma = \left\{\Sigma_{ij}\right\}_{1\le i,j\le M} = \hat{\rho}_{ij}\hat{\sigma}_i\hat{\sigma}_j. \tag{10}$$

Under the proposed transformation payoff function takes the form

$$\varphi(\mathbf{S}) = \varphi\left(E(e^{x_1}, e^{x_2}, \dots, e^{x_M})\right) = \phi(X). \tag{11}$$

2.2 | American options

In contrast to European options, American ones can be exercised at any moment prior to the maturity T. Mathematically speaking, it leads the Equation (6) to the following partial integro-differential complementarity problem [3]:

$$\begin{cases} U_\tau(X,\tau) \ge \mathcal{D}U(X,\tau) + \mathcal{I}U(X,\tau), \\ U(X,\tau) \ge \phi(X), \\ (U(X,\tau) - \phi(X))\,(U_\tau(X,\tau) - \mathcal{D}U(X,\tau) - \mathcal{I}U(X,\tau)) = 0 \end{cases} \tag{12}$$

for $X \in \mathbb{R}^M$ and $\tau \in (0, T]$.

The American option pricing is formulated as an optimal stopping problem [27], however, there are empirical evidences of irrational exercises [28]. These aspects have been treated in Gad and Pedersen [29] by developing a model with rationality parameter. This model has been used in put options valuation under classical Black–Scholes model [30] and under the regime-switching [31]. In present paper, we extend this rational behavior approach to the multidimensional jump-diffusion models.

Following the ideas of previous works [30, 31], let us introduce the rationality parameter Λ_{Rat}, such that $\Lambda_{\text{Rat}} = 0$ provides the price of the corresponding European option (no early exercise), and large values of Λ_{Rat} allows the approximation of the American option with rational exercise. Then, the irrational behavior of the trader is modeled throughout the intensity function $\boldsymbol{\Phi}$:

$$\boldsymbol{\Phi}(\gamma) = \begin{cases} \Lambda_{\text{Rat}}, & \text{if}\, \gamma \ge 0, \\ 0, & \text{otherwise.} \end{cases} \tag{13}$$

Remark 1. The intensity function (13) can be written as follows:

$$\boldsymbol{\Phi}(\gamma) = \Lambda_{\text{Rat}}\mathbf{1}_{(\gamma\ge 0)}, \tag{14}$$

where $\mathbf{1}_{(\gamma\ge 0)}$ is the indicator function. The intensity function (13) corresponds to the penalty method for the free-boundary problem and can be interpreted as the willing of a buyer to exercise the option when it is profitable [30].

Remark 2. The choice of the intensity function is not unique; in Company et al. [30], several smooth analogs of the stepwise function (13) have been proposed.

After the logarithmic transformation (5), the transformed option price of the American option is the solution of the following PIDE:

$$U_\tau(X,\tau) = \mathcal{D}U(X,\tau) + \mathcal{I}U(X,\tau) + \mathcal{R}U(X,\tau), \tag{15}$$

where $\mathcal{D}U(X,\tau)$ and $\mathcal{I}U(X,\tau)$ are defined in (7) and (8), respectively, and $\mathcal{R}U(X,\tau)$ is the rationality term given by

$$\mathcal{R}U(X,\tau) = \boldsymbol{\Phi}\left(U(X,0) - U(X,\tau)\right)\cdot\left(U(X,0) - U(X,\tau)\right). \tag{16}$$

Since the choice of the rationality parameter Λ_{Rat} allows the evaluation of both, European and American options, further we consider more general PIDE (15). Note that the European option value corresponds to $\Lambda_{\text{Rat}} = 0$.

10991476, 2023, 9, Downloaded from https://onlinelibrary.wiley.com/doi/10.1002/mma.9125 by Universidad De Cantabria, Wiley Online Library on [16/05/2023]. See the Terms and Conditions (https://onlinelibrary.wiley.com/terms-and-conditions) on Wiley Online Library for rules of use; OA articles are governed by the applicable Creative Commons License

3 | MIXED DERIVATIVE REMOVING

We start this section by recalling the previous results:

Theorem 1 (Company et al., [21]). *Let $R = \left\{\rho_{ij}\right\}_{1\le i,j\le M}$ be the symmetric positive semi-definite matrix and let L, P and D be matrices in $\mathbb{R}^{M\times M}$ satisfying*

$$PRP^T = LDL^T. \tag{17}$$

Then, the transformation

$$Y = CX \in \mathbb{R}^M,\ C = L^{-1}P, \tag{18}$$

leads the differential operator (7) to the canonical form without the mixed derivative terms.

By denoting $W(Y,\tau) = U(X,\tau)$, under the transformation (18), differential operator (7) takes the following form:

$$\mathcal{D}W = \frac{1}{2}\sum_{i=1}^{M} d_{ii}\frac{\partial^2 W}{\partial y_i^2} + \sum_{i=1}^{M}\left(\sum_{j=1}^{M}\left(r - q_j - \lambda\kappa_j - \frac{\sigma_j^2}{2}\right)c_{ij}\right)\frac{\partial W}{\partial y_i} - (r+\lambda)W, \tag{19}$$

where c_{ij} are the entries of the transformation matrix C, d_{ii} are the diagonal elements of the matrix D.

Remark 3 (Company et al., [21]). Under the transformation (18), differential operator (7) can be written in the compact form

$$\mathcal{D}W = \frac{1}{2}(D\nabla)\cdot\nabla W + (CQ)\cdot\nabla W - (r+\lambda)W, \tag{20}$$

where $Q = (Q_1, Q_2, \dots, Q_M)^T$ with $Q_j = \left(r - q_j - \lambda\kappa_j - \frac{\sigma_j^2}{2}\right)$, $1 \le j \le M$.

Due to (18), the integral term (8) will also change by taking as new integrating variable

$$\boldsymbol{\xi} = Y + C\boldsymbol{\eta} \iff \boldsymbol{\eta} = C^{-1}(\boldsymbol{\xi} - Y) \tag{21}$$

with the Jacobian

$$|\mathcal{J}| = \det\left\{\frac{\partial \eta_i}{\partial \xi_j}\right\} = \frac{1}{\det C}, \tag{22}$$

resulting in the following:

$$\mathcal{I}W = \frac{\lambda}{\det C}\int_{\mathbb{R}^M} W(\boldsymbol{\xi},\tau)g\left(C^{-1}(\boldsymbol{\xi} - Y)\right)d\boldsymbol{\xi}, \tag{23}$$

where $g(\cdot)$ is defined in (9).

Finally, the PIDE to solve is written as follows:

$$W_\tau(Y,\tau) = \mathcal{D}W(Y,\tau) + \mathcal{I}W(Y,\tau) + \mathcal{R}W(Y,\tau),\ Y \in \mathbb{R}^M,\ \tau \in [0,T], \tag{24}$$

where the differential operator is defined in (19), the integral term is given in (23) and $\mathcal{R}W(Y,\tau)$ stands for corresponding penalty term.

4 | NUMERICAL SOLUTION

Multidimensional PIDE (24) is solved numerically. In the present paper, we propose a combination of the ETD method with the Gauss–Hermite quadrature. For the differential operator discretization, the second order centered FD approximation is used.

As the initial condition, the transformed payoff function (11) is used setting $X = C^{-1}Y$.

For the numerical solution, the infinite theoretical domain is truncated; thus, the boundaries of this new truncated domain are the interior points of the theoretical domain, and thus, the Equation (24) holds. Since the numerical solution is calculated step by step starting from the initial condition capturing the payoff of the problem, the type of the option is taken into account also at the boundaries of the truncated numerical domain.

10991476, 2023, 9, Downloaded from https://onlinelibrary.wiley.com/doi/10.1002/mma.9125 by Universidad De Cantabria, Wiley Online Library on [16/05/2023]. See the Terms and Conditions (https://onlinelibrary.wiley.com/terms-and-conditions) on Wiley Online Library for rules of use; OA articles are governed by the applicable Creative Commons License

4.1 | Differential operator discretization

Following the ideas of Company et al. [32], we consider the truncated domain $\Omega = \left[y_{1_{\min}}, y_{1_{\max}}\right] \times \ldots \times \left[y_{M_{\min}}, y_{M_{\max}}\right]$ and introduce the uniform in each dimension mesh

$$y_i^j = y_{i_{\min}} + jh_i,\ h_i = \frac{1}{N_i}(y_{i_{\max}} - y_{i_{\min}}),\ j = 0, \ldots, N_i,\ i = 1, \ldots, M. \tag{25}$$

Note that the total number of spatial nodes

$$N + 1 = \prod_{i=1}^{M}(N_i + 1). \tag{26}$$

Let us number all nodes from 0 to N, such that $(y^j, \tau) = (y_1^{j_1}, y_2^{j_2}, \ldots, y_M^{j_M}, \tau)$, where

$$j = [j_1, j_2, \ldots, j_M] = j_1 + \sum_{i=2}^{M}\left(\prod_{n=1}^{i-1}(N_n + 1)\right) j_i. \tag{27}$$

The boundary nodes $y^j \in \partial\Omega$ are the nodes with at least one of the indexes j_i, $i = 1, \ldots, M$, equal to zero or N_i, that is,

$$\partial\Omega = \left\{(y_1^{j_1}, y_2^{j_2}, \ldots, y_M^{j_M}) :\ \exists m, 1 \le m \le M, \text{ such that } j_m = 0, \text{ or } j_m = N_m\right\}. \tag{28}$$

The set of indexes of all boundary and interior nodes are denoted by Γ and $\bar{\Gamma}$, respectively.

Then, the approximate solution at the node (y^j, τ) is denoted by $u_{j_1, \ldots, j_M}(\tau)$. Further for the simplicity of the presentation, let us use the abbreviated notation mentioning only the index of the changing variable y_i, the rest of indexes keep the value, and then, the spatial derivatives at the interior nodes are approximated as follows:

$$\frac{\partial W}{\partial y_i}(y^j, \tau) = \frac{u_{j_i+1}(\tau) - u_{j_i-1}(\tau)}{2h_i} + O(h_i^2), \tag{29}$$

$$\frac{\partial^2 W}{\partial y_i^2}(y^j, \tau) = \frac{u_{j_i+1}(\tau) - 2u_{j_i}(\tau) + u_{j_i-1}(\tau)}{h_i^2} + O(h_i^2). \tag{30}$$

At the boundaries, the Equation (24) holds; thus, the discretization of the spatial derivatives is established as follows: for $i = 1, \ldots, M$, $j = 0, \ldots, N$,

$$\frac{\partial W}{\partial y_i}(y^j, \tau) = \frac{-3u_{j_i}(\tau) + 4u_{j_i+1}(\tau) - u_{j_i+2}(\tau)}{2h_i} + O(h_i^2), j_i = 0, \tag{31}$$

$$\frac{\partial W}{\partial y_i}(y^j, \tau) = \frac{3u_{j_i}(\tau) - 4u_{j_i-1}(\tau) + u_{j_i-2}(\tau)}{2h_i} + O(h_i^2), j_i = N_i, \tag{32}$$

$$\frac{\partial^2 W}{\partial y_i^2}(y^j, \tau) = \frac{2u_{j_i}(\tau) - 5u_{j_i+1}(\tau) + 4u_{j_i+2}(\tau) - u_{j_i+3}(\tau)}{h_i^2} + O(h_i^2), j_i = 0, \tag{33}$$

$$\frac{\partial^2 W}{\partial y_i^2}(y^j, \tau) = \frac{2u_{j_i}(\tau) - 5u_{j_i-1}(\tau) + 4u_{j_i-2}(\tau) - u_{j_i-3}(\tau)}{h_i^2} + O(h_i^2), j_i = N_i. \tag{34}$$

Substituting the derivatives in (19) by the finite-difference approximations (29)–(30) at the interior nodes, and (31)–(34) at the boundaries of the computational domain, the differential operator $\mathcal{D}W$ (19) is transformed to the matrix operator $A\mathbf{u}$, where $\mathbf{u} = [u_0, \ldots, u_N]^T$, $A = (a_{ij})_{0 \le i,j \le N}$ is a sparse matrix with the following nonzero entries:

1. For the interior nodes $j \in \bar{\Gamma}$:

$$a_{jj} = -2\sum_{i=1}^{M}\frac{d_{ii}}{h_i^2} - (r + \lambda),\ a_{j,j\pm m} = \frac{d_{mm}}{h_m^2} \pm \frac{1}{2h_i}\alpha_m, \tag{35}$$

10991476, 2023, 9, Downloaded from https://onlinelibrary.wiley.com/doi/10.1002/mma.9125 by Universidad De Cantabria, Wiley Online Library on [16/05/2023]. See the Terms and Conditions (https://onlinelibrary.wiley.com/terms-and-conditions) on Wiley Online Library for rules of use; OA articles are governed by the applicable Creative Commons License

where $m = \prod_{n=1}^{i-1}(N_n + 1)$, $i = 1, \dots, M$, and

$$\alpha_m = \sum_{i=1}^{M} \left(r - q_i - \lambda\kappa_i - \frac{\sigma_i^2}{2} \right) c_{mi}. \tag{36}$$

2. For the lower boundary nodes $j \in \Gamma$, $j_m = 0$:

$$a_{jj} = 2\sum_{i=1}^{M} \frac{d_{ii}}{h_i^2} - 3\frac{\alpha_j}{2h_j} - (r + \lambda), \tag{37}$$

$$a_{j,j+m} = -5\frac{d_{jj}}{h_j^2} + 4\frac{\alpha_j}{2h_j}, \tag{38}$$

$$a_{j,j+2m} = 4\frac{d_{jj}}{h_j^2} - \frac{\alpha_j}{2h_j}, \tag{39}$$

$$a_{j,j+3m} = -\frac{d_{jj}}{h_j^2}, \tag{40}$$

where $m = \prod_{n=1}^{i-1}(N_n + 1)$, $i = 1, \dots, M$, and α_m are defined by (36).

3. For the upper boundary, $j \in \Gamma$, $j_m = N_m$:

$$a_{jj} = 2\sum_{i=1}^{M} \frac{d_{ii}}{h_i^2} + 3\frac{\alpha_j}{2h_j} - (r + \lambda), \tag{41}$$

$$a_{j,j-m} = -5\frac{d_{jj}}{h_j^2} - 4\frac{\alpha_j}{2h_j}, \tag{42}$$

$$a_{j,j-2m} = 4\frac{d_{jj}}{h_j^2} + \frac{\alpha_j}{2h_j}, \tag{43}$$

$$a_{j,j-3m} = -\frac{d_{jj}}{h_j^2}, \tag{44}$$

where $m = \prod_{n=1}^{i-1}(N_n + 1)$, $i = 1, \dots, M$ and α_m are defined by (36).

4.2 | ETD method

After the semi-discretization of the differential operator described above, the PIDE (24) is substituted by the system of the ordinary differential equations:

$$\frac{d\boldsymbol{u}}{d\tau} = A\boldsymbol{u} + \boldsymbol{F}(\boldsymbol{u}(\tau)), \tag{45}$$

where A is a sparse banded $(N + 1) \times (N + 1)$ matrix of the coefficients (35)–(44); $\boldsymbol{F}$ is a vector-function on the $\boldsymbol{u}$, which contains the approximation of the integral term (23) and the penalty term at each point of the mesh y^j at the moment τ. The approximation of $\mathcal{I}W$ will be discussed in the following subsection.

System (45) can be solved by an ETD method [23] basing on the matrix exponential. Firstly, we introduce a uniform temporal mesh with step-size $k = \frac{T}{N_\tau}$, such that

$$t^n = nk, \ n = 0, \dots, N_\tau - 1. \tag{46}$$

10991476, 2023, 9, Downloaded from https://onlinelibrary.wiley.com/doi/10.1002/mma.9125 by Universidad De Cantabria, Wiley Online Library on [16/05/2023]. See the Terms and Conditions (https://onlinelibrary.wiley.com/terms-and-conditions) on Wiley Online Library for rules of use; OA articles are governed by the applicable Creative Commons License

In Cox and Matthews [23], it has been shown that the exact solution of (45) in the interval $[t^n, t^{n+1}]$ can be found as

$$\boldsymbol{u}(t^{n+1}) = e^{Ak}\boldsymbol{u}(t^n) + \int_0^k e^{As}\boldsymbol{F}(\boldsymbol{u}(t^{n+1} - s))ds. \tag{47}$$

Note that the integrand in (47) depends on the solution at unknown time-level t^{n+1}; thus, in order to obtain the explicit scheme, we approximate these unknown values by the corresponding $\boldsymbol{u}(t^n)$, then $\boldsymbol{F}(\boldsymbol{u}(t^n))$ is independent on integration variable s, and one gets an approximation of order $\mathcal{O}(k^2)$ [23],

$$\boldsymbol{u}(t^{n+1}) \approx e^{Ak}\boldsymbol{u}(t^n) + \left(\int_0^k e^{As}ds\right)\boldsymbol{F}(\boldsymbol{u}(t^n)). \tag{48}$$

In order to avoid the computation of matrix inverse A^{-1}, which can be challenging due to the dimension of the matrix A, and moreover, its singularity or ill-conditioning, we approximate the integral term in (48) by the Simpson's rule whose error of approximation is $\mathcal{O}(k^5)$ [33]. Denoting the approximate solution at t^n by $\boldsymbol{u}^n \approx \boldsymbol{u}(t^n)$, one gets the following explicit formula for computation of $\boldsymbol{u}^{n+1}$:

$$u^{n+1} = e^{Ak}\boldsymbol{u}^n + \frac{k}{6}\left(I + 4e^{Ak/2} + e^{Ak}\right)\boldsymbol{F}(\boldsymbol{u}^n),\ n = 0, \dots, N_\tau - 1. \tag{49}$$

where I is the identity $(N+1)\times(N+1)$ matrix. Note that the matrix A is constant-values; thus, the corresponding matrix exponential e^{Ak} and $e^{Ak/2}$ are constant-values as well and can be computed just before the temporal iterations. Further, we discuss the numerical approximation of the non-linear (integral) term $\boldsymbol{F}(\boldsymbol{u}^n)$.

4.3 | Multivariate Gauss–Hermite quadrature

The non-linear term $\boldsymbol{F}(\boldsymbol{u}^n)$ contains the discretization of the integral term $\mathcal{I}W$ and the penalty term $\mathcal{R}W$, and it can be represented as the sum of two vector operators $\boldsymbol{F}(\boldsymbol{u}^n) = \boldsymbol{F}_I(\boldsymbol{u}^n) + \boldsymbol{F}_R(\boldsymbol{u}^n)$. Hence, the discretization of the integral term is written as follows:

$$\boldsymbol{F}_I(\boldsymbol{u}^n) \approx \frac{\lambda}{\det C}\int_{\mathbb{R}^M} u(\boldsymbol{\xi}, t^n)g\left(C^{-1}(\boldsymbol{\xi} - Y)\right)d\boldsymbol{\xi}, \tag{50}$$

which can be approximated by some numerical integration method, such as multivariate trapezoidal rule, as it is used for two-asset case in Boen and Hout [3] or Gaussian quadrature (for bi-variate Gauss–Hermite quadrature, see [14]).

The main advantage of the trapezoidal rule is its simplicity and applicability for any meshes. However, for good accuracy, a huge amount of the integrand evaluation is needed. In the case of higher dimensions (more than 2), it is computationally costly. Thus, in this paper, we focus on the multivariate Gauss quadrature [34], which is a very potent alternative to costly Newton–Cotes composite rules or slowly convergent Monte Carlo methods. In fact, four-nodes Gauss–Hermite quadrature used in present study is found to be optimal due to high accuracy and low computational cost.

In the case of one dimension, the Gauss–Hermite quadrature of N_{GH} nodes is written as

$$\int_{-\infty}^{\infty} f(x)dx \approx \sum_{j=1}^{N_{GH}} \omega_j f(\xi_j)\exp(\xi_j^2), \tag{51}$$

where ξ_j, $j = 1, \dots, N_{GH}$ are the roots of the physicist's version of the Hermite polynomials and ω_j are the associated weights. For $N_{GH} = 4$ the nodes ξ_j and weights ω_j are given in Table 1.

TABLE 1 The nodes and weights of the Gauss–Hermite quadrature for $N_{GH} = 4$.

Nodes ξ_j	Weights ω_j
±1.6506801238857845558 83	0.08131283544724517714 3
±0.5246476232752903178841	0.8049140900055128365061

10991476, 2023, 9, Downloaded from https://onlinelibrary.wiley.com/doi/10.1002/mma.9125 by Universidad De Cantabria, Wiley Online Library on [16/05/2023]. See the Terms and Conditions (https://onlinelibrary.wiley.com/terms-and-conditions) on Wiley Online Library for rules of use; OA articles are governed by the applicable Creative Commons License

In 2D case, the previous formula is extended to the following result:

$$\int_{-\infty}^{\infty}\int_{-\infty}^{\infty} f(x,y)dxdy \approx \sum_{j_1=1}^{N_{GH}}\sum_{j_2=1}^{N_{GH}} \omega_{j_1}\omega_{j_2} f(\xi_{j_1},\xi_{j_2})\exp(\xi_{j_1}^2+\xi_{j_2}^2), \tag{52}$$

where the nodes ξ_{j_1} and ξ_{j_2} and associated weights $\omega_{j_1}, \omega_{j_2}$ are also given in Table 1 for $N_{GH} = 4$.

Expanding this formula for the case of M variables, one gets the approximation of the non-linear term in (49),

$$\begin{aligned}
\boldsymbol{F}_I(\boldsymbol{u}^n) &\approx \frac{\lambda}{\det C}\int_{\mathbb{R}^M} u(\boldsymbol{\xi},t^n) g\left(C^{-1}(\boldsymbol{\xi}-Y)\right) d\boldsymbol{\xi} \\
&\approx \frac{\lambda}{\det C}\int_{-\infty}^{\infty}\dots\int_{-\infty}^{\infty} u(\boldsymbol{\xi},t^n) g\left(C^{-1}(\boldsymbol{\xi}-Y)\right) d\xi_1\ \dots\ d\xi_M, \\
&\approx \frac{\lambda}{\det C}\sum_{j_1=1}^{N_{GH}}\sum_{j_2=1}^{N_{GH}}\dots\sum_{j_M=1}^{N_{GH}} \omega_{j_1}\omega_{j_2}\ \dots\ \omega_{j_M} u(\boldsymbol{\xi}^j,t^n) g\left(C^{-1}((\boldsymbol{\xi}^j)^T-Y)\right)\exp(\xi_{j_1}^2+\ \dots\ +\xi_{j_M}^2),
\end{aligned} \tag{53}$$

where $\boldsymbol{\xi}^j = [\xi_{j_1},\ \dots\ ,\xi_{j_M}]$, are vectors of all possible combinations of the nodes of the one-dimensional GH quadrature from Table 1.

In the formula above, the solution at the node $\boldsymbol{\xi}^j$ is required, which may differ from the mesh-points y^j; thus, multivariate linear interpolation is employed.

4.4 | Multi-linear interpolation

Let us denote the query point by $\boldsymbol{\zeta}$. In order to minimize the error, we start with searching for the nearest to $\boldsymbol{\zeta}$ mesh-nodes denoted by Y^0 and Y^1, that is, the coordinates of these nodes satisfy

$$Y_i^0 \le \zeta_i \le Y_i^1,\ \forall i = 1,\ \dots\ ,M. \tag{54}$$

Analogously to bi-linear or tri-linear interpolation, we consider M-dimensional hypercube with 2^M corners denoted by δ, which can be numbered by binary vectors of the length M, where the index $[0,\ \dots\ ,0]$ corresponds to $\delta_{0,\dots,0} = Y^0$ and the index $[1,\ \dots\ ,1]$ corresponds to $\delta_{1,\dots,1} = Y^1$. The i-th component in the index equal to 1 means that the i-th component of the corresponding corner is Y_i^1, and Y_i^0, otherwise.

Now, let us introduce a function $\boldsymbol{\Xi}$, which transforms a M-dimensional vector δ to 2^M-dimensional:

$$\boldsymbol{\Xi}(\delta) = \left[1, \delta_1,\ \dots\ ,\delta_M, \delta_1\delta_2,\ \dots\ ,\delta_1\delta_M, \delta_2\delta_3,\ \dots\ ,\delta_1\delta_2\delta_3,\ \dots\ ,\left(\prod_{i=1}^{M}\delta_i\right)\right]. \tag{55}$$

Then the solution of the multi-linear interpolation problem can be written as

$$u(\boldsymbol{\zeta}) = \boldsymbol{\alpha}\cdot\boldsymbol{\Xi}(\boldsymbol{\zeta})^T, \tag{56}$$

where $\boldsymbol{\alpha} = [\alpha_0,\ \dots\ ,\alpha_{2^M}]$ is the vector of the coefficients, and

Coefficients $\boldsymbol{\alpha}$ are found as the solution of the following linear system:

$$\begin{pmatrix} \boldsymbol{\Xi}\left(\delta_{0,\dots,0,0}\right) \\ \boldsymbol{\Xi}\left(\delta_{0,\dots,0,1}\right) \\ \boldsymbol{\Xi}\left(\delta_{0,\dots,0,1}\right) \\ \dots \\ \boldsymbol{\Xi}\left(\delta_{1,\dots,1,1}\right) \end{pmatrix}\begin{pmatrix} \alpha_0 \\ \alpha_1 \\ \alpha_2 \\ \dots \\ \alpha_{2^M} \end{pmatrix} = \begin{pmatrix} u\left(\delta_{0,\dots,0,0}\right) \\ u\left(\delta_{0,\dots,0,1}\right) \\ u\left(\delta_{0,\dots,0,1}\right) \\ \dots \\ u\left(\delta_{1,\dots,1,1}\right) \end{pmatrix}. \tag{57}$$

10991476, 2023, 9, Downloaded from https://onlinelibrary.wiley.com/doi/10.1002/mma.9125 by Universidad De Cantabria, Wiley Online Library on [16/05/2023]. See the Terms and Conditions (https://onlinelibrary.wiley.com/terms-and-conditions) on Wiley Online Library for rules of use; OA articles are governed by the applicable Creative Commons License

5 | NUMERICAL RESULTS

Apart from the new combined multivariate GH-ETD method for non-linear PIDE, we propose the algorithm which can treat any kind of options. It is possible because no additional boundary conditions are posed, which are different for different kind of options. In order to prove the adaptability of the proposed scheme, we start this section with various exotic options on two assets. Then, we focus on the multi-asset jump-diffusion models.

For most of the examples, we chose uniform grid with $N = 150$ nodes in each direction. Thus, the size of matrix A is $N^2 \times N^2$. In order to perform such huge matrix calculations, sparse matrices and parallel computing tools of MATLAB are used. Moreover, the matrix exponential in this case is time-consuming, which urges an effective and fast algorithm. For the calculations, algorithm proposed in previous studies [35, 36] is employed.

Computations are performed by MATLAB R2021a for Windows 10 home (64-bit) Intel(R) Core(TM) i5-8265u CPU, 1.60 GHz.

5.1 | American options

Let us consider the case of American basket call option with the payoff function

$$\varphi_{\text{basket}}(\mathbf{S}) = \max\left\{\sum_{i=1}^{M} \alpha_i S_i - E, 0\right\}, \tag{58}$$

where α_i, $i = 1, \dots, M$, are the basket weights, such as $\sum_{i=1}^{M} \alpha_i = 1$.

American options give the opportunity of the early exercise, thus rationality formulation (15) is considered. The rationality parameter is set $\Lambda_{\text{Rat}} = 100$ (in previous study the convergence to American option price was proven [30]).

Example 5.1 (American basket call)**.** Consider an American basket call option [32] with the parameters given in Table 2.

For better approximation the spatial computational domain is chosen as $[-5, 5] \times [-5, 5]$ with 150×150 nodes. In Table 3, we compare the results for $(S_1, S_2) = (100, 100)$ with ones computed by the FD method (with mixed derivative removing transformation) proposed in Company et al. [32] and by the high-order computational (HOC) method of [26]. The option price for other assets' prices are reported in Table 4. The numerical solution is plotted in Figure 1.

5.2 | Options under jump-diffusion model

Example 5.2. (1D American option 12,19,24)**.** We consider 1D American option, both put and call, under Merton's jump-diffusion model with parameters given in Table 5.

The numerical solution is plotted in Figure 2: the black solid line represents the payoff, while the solution at $t = 0$ is presented by the blue dashed line. In order to obtain better approximation, 60-nodes Gauss–Hermite quadrature is

TABLE 2 Parameters for the American basket option.

T	E	r	q_1	q_2	σ_1	σ_2	ρ
6 months	100	0.03	0.01	0.01	0.12	0.14	0.3

TABLE 3 Price of American basket call option with parameters given in Table 2 for $(S_1, S_2) = (100, 100)$.

Method	Option price
FD method [32]	3.41344
HOC [26]	3.35094
GH-ETD	3.45546

TABLE 4 The price of American basket call option with parameters given in Table 2.

	S_1		
S_2	90	100	110
90	0.3302	1.2856	3.4288
100	1.3165	3.4555	6.8729
110	3.4966	6.8972	11.2116

10991476, 2023, 9, Downloaded from https://onlinelibrary.wiley.com/doi/10.1002/mma.9125 by Universidad De Cantabria, Wiley Online Library on [16/05/2023]. See the Terms and Conditions (https://onlinelibrary.wiley.com/terms-and-conditions) on Wiley Online Library for rules of use; OA articles are governed by the applicable Creative Commons License

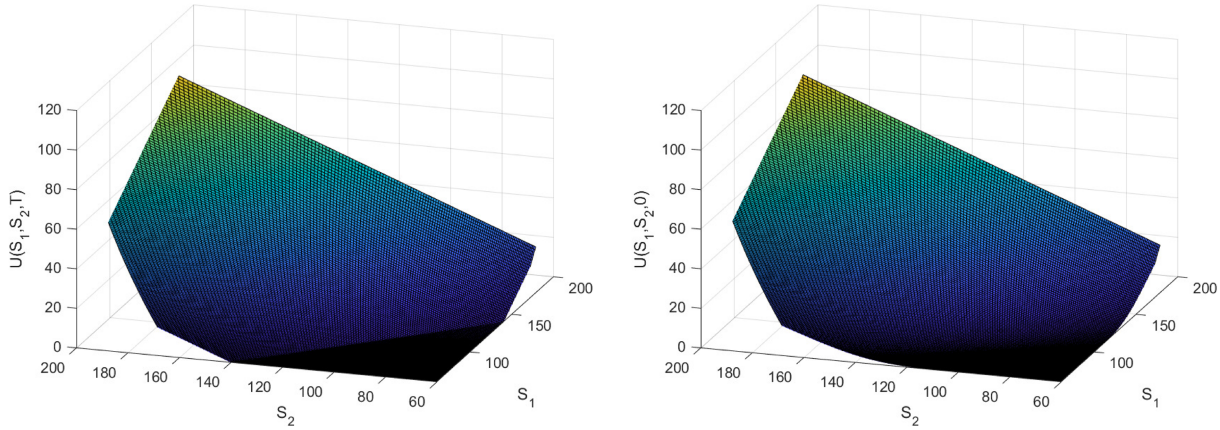

FIGURE 1 The price of American basket call option with parameters given in Table 2 at $t = T$ (payoff) (left) and $t = 0$ (right). [Colour figure can be viewed at wileyonlinelibrary.com]

T	E	r	q	σ	λ	μ	$\hat{\sigma}$
3 months	100	0.05	0.0	0.15	0.1	−0.9	0.45

TABLE 5 Parameters for the American option under Merton's jump-diffusion model.

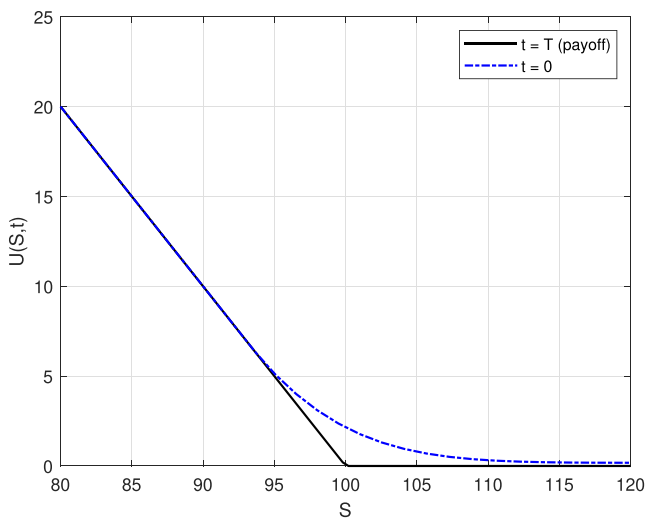

FIGURE 2 Option price at the maturity, $t = T$, (black solid line) and at $t = 0$ (blue dashed line) for the American put under the jump-diffusion model with parameters given in Table 5. [Colour figure can be viewed at wileyonlinelibrary.com]

employed, which requires larger computational domain. Thus, the infinite domain is truncated by [−10,10]. To perform more accurate computation, the number of spatial nodes is set $N = 500$. Rationality parameter is chosen $\Lambda_{\text{Rat}} = 100$.

This example is considered in many papers [12, 19, 24, 37], which allows us to compare the results. The option values at $S = 100$ computed by the front-fixing with ETD (FF-ETD) method of Company et al. [25], radial basis function with differential quadrature with exponential time integration (RBF-ETI) of aib et al. [19], implicit method by d'Halluin et al. [37], and the proposed method are reported in Table 6.

Example 5.3. Now, let us consider a European put option on the minimum of two assets S_1, S_2 as it is done in the literature [14, 22]. Parameters are given in Table 7.

In this case $M = 2$, the payoff function is written as follows:

$$\varphi(S_1, S_2) = \max\{E - \min\{S_1, S_2\}, 0\}. \tag{59}$$

10991476, 2023, 9, Downloaded from https://onlinelibrary.wiley.com/doi/10.1002/mma.9125 by Universidad De Cantabria, Wiley Online Library on [16/05/2023]. See the Terms and Conditions (https://onlinelibrary.wiley.com/terms-and-conditions) on Wiley Online Library for rules of use; OA articles are governed by the applicable Creative Commons License

TABLE 6 American put option value at $S = 100$ computed by various methods.

Method	Option price
FF-ETD [24]	3.2428
RBF-ETI [19]	3.2418
Implicit method [37]	3.2412
GH-ETD	3.2408

TABLE 7 Parameters for the European put on minimum of two assets.

T	E	r	q_1	q_2	σ_1	σ_2	ρ	λ	μ_1	μ_2	$\hat{\sigma}_1$	$\hat{\sigma}_2$	$\hat{\rho}$
1 year	100	0.05	0.0	0.0	0.12	0.15	0.3	0.6	−0.1	0.1	0.17	0.13	−0.2

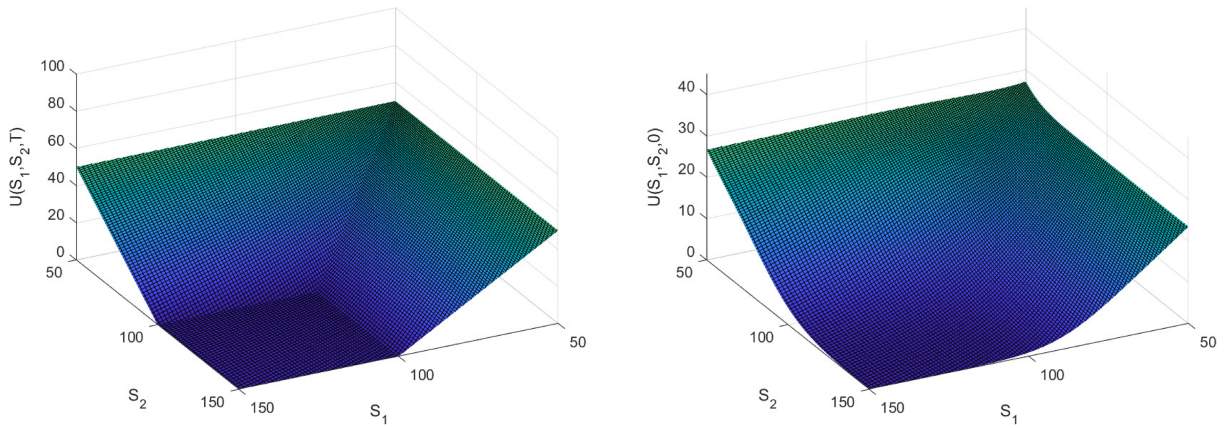

FIGURE 3 Option price at the maturity (left) and at $t = 0$ (right) for the European put on the minimum of two assets with parameters given in Table 7 (numerical solution by the proposed combined GH-ETD method). [Colour figure can be viewed at wileyonlinelibrary.com]

We apply the logarithmic transformation (5) and the mixed derivative removing. The transformation matrix C is calculated by Theorem 1, resulting in the following:

$$C = \begin{pmatrix} 8.3333 & 0 \\ -2.5000 & 6.6667 \end{pmatrix}, \ \det C = 55.5556 \neq 0. \tag{60}$$

We consider the truncated domain $[-100, 10] \times [-100, 10]$ with the uniform mesh of $N_1 = N_2 = 100$ spatial nodes, $k = 0.1$. The matrix exponential is computed by the fast algorithm [35, 36].

Payoff and the numerical solution computed by the proposed combined GH-ETD method are presented in Figure 3. In order to compare the results with ones in Clift and Forsyth [22], we use the bi-linear interpolation to approximate the solution at $[S_1, S_2] = \{90, 100, 110\}$. The results are reported in Table 8.

Now, let us check how the price changes in the case of American option.

Example 5.4. We consider the put-on-min with parameters given in Table 7.

Instead of the LCP problem and penalty method, as it is proposed in previous works [3, 14], we include the rationality term and consider the numerical solution of the Equation (15) with $\Lambda_{\text{Rat}} = 100$. The numerical solution (at $t = 0$) is presented in Figure 4.

The GH quadrature with 4 nodes is used which allows fast and accurate solution. Comparing right plots of Figures 3 and 4, one can notice that the American option value is higher than European one which agrees with theoretical results. Moreover, for small asset prices (at the lower boundaries) the price of American option coincides with the payoff. It is explained by the fact that the optimal exercise boundary leads in the computational domain.

One of the computational challenges of the proposed algorithm is computing and storage of the matrix exponential. In present work, the fast and efficient algorithm [35, 36] is employed. This algorithm admits parallel computing and sparse matrices, which allows us to significantly reduce the computational cost. The CPU-time and memory complexity are reported in Table 9.

The proposed method can be used for higher-dimensional problems. As an example, let us consider the option with three correlated underlying assets.

10991476, 2023, 9, Downloaded from https://onlinelibrary.wiley.com/doi/10.1002/mma.9125 by Universidad De Cantabria, Wiley Online Library on [16/05/2023]. See the Terms and Conditions (https://onlinelibrary.wiley.com/terms-and-conditions) on Wiley Online Library for rules of use; OA articles are governed by the applicable Creative Commons License

TABLE 8 The price of the European put-on-min option with the parameters given in Table 7.

	S_1		
S_2	90	100	110
90	15.9578	13.5532	12.2341
100	12.1804	9.1420	7.5620
110	9.9008	6.4407	4.6335

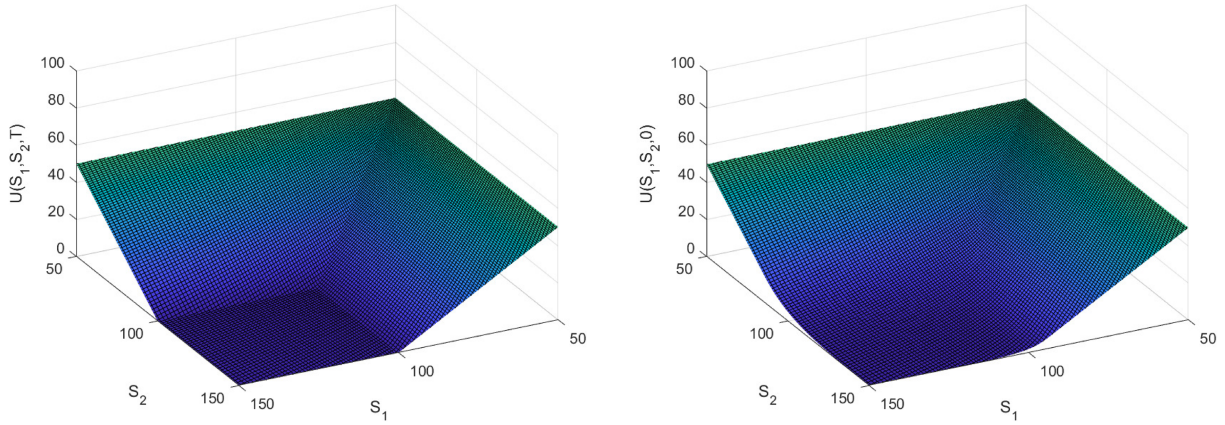

FIGURE 4 Option price at the maturity (left) and at $t = 0$ (right) for the American put on the minimum of two assets with parameters given in Table 7 (numerical solution by the proposed combined GH-ETD method). [Colour figure can be viewed at wileyonlinelibrary.com]

TABLE 9 CPU-time for the matrix exponential computation and the memory occupied by the resulting array for the American put-on-min option with the parameters given in Table 7.

N	CPU-Time, s	Memory, MB
50	0.3112	9.9
100	3.3750	61
150	9.6250	141
200	13.0469	256
250	22.7969	404
300	29.6094	589

TABLE 10 Parameters for the three-asset (without dividend, $q_1 = q_2 = q_3 = 0$) American option.

T	E	r	σ_1	σ_2	σ_3	μ_1	μ_2	μ_3	$\hat{\sigma}_1$	$\hat{\sigma}_2$	$\hat{\sigma}_3$	$\rho_{J_{1,2}}$	$\rho_{J_{1,3}}$	$\rho_{J_{2,3}}$
1 year	40	0.05	0.25	0.30	0.20	-0.10	0.10	0.10	0.17	0.13	0.10	-0.20	0.10	0.20

TABLE 11 American 3D basket option price at $(S_1, S_2, S_3) = (40, 35, 35)$ computed at different meshes and by using 4, 8 and 10 nodes of GH-quadrature.

	N_{GH}		
(h, k)	4	8	10
(0.5, 0.25)	23.2461	23.2461	23.2461
(0.25, 0.0625)	23.8436	23.8436	23.8436
(0.15, 0.0225)	23.9418	23.9418	23.9418

Example 5.5. A three-asset American option is considered under the jump-diffusion model with the parameters given in Table 10, $\lambda = 0.6$, and the correlation matrix

$$R = \begin{pmatrix} 1.0 & 0.9 & 0.9 \\ 0.9 & 1.0 & 0.8 \\ 0.9 & 0.8 & 1.0 \end{pmatrix}. \tag{61}$$

The numerical solution is constructed in the 3D-spatial domain $[-10, 5] \times [-10, 5] \times [-10, 5]$ with various number of spatial nodes; the time-step is chosen as $k = h^2$ (h is the same for all dimensions). The option price at $(S_1, S_2, S_3) = (40, 35, 35)$ for various grade of GH quadrature are reported in Table 11.

From Table 11, one can observe that the solution converges to the option value 23.0017 with increasing number of mesh points (decreasing step sizes).

10991476, 2023, 9, Downloaded from https://onlinelibrary.wiley.com/doi/10.1002/mma.9125 by Universidad De Cantabria, Wiley Online Library on [16/05/2023]. See the Terms and Conditions (https://onlinelibrary.wiley.com/terms-and-conditions) on Wiley Online Library for rules of use; OA articles are governed by the applicable Creative Commons License

6 | CONCLUSIONS

This paper has proposed the universal numerical algorithm for various option pricing models. It is based on the preliminary mixed derivative eliminating transformation, which simplifies the computational stencil and improves the stability conditions of the numerical scheme. The transformed PIDE problem is established on the infinite domain. The numerical solution is then constructed on the truncated domain by applying for the spatial discretization the finite difference schemes of the second order.

The numerical scheme adopts to any kind and style of option due to the one-sided finite differences used at the boundary points. Thus, no boundary conditions are needed, we assume that the PIDE is valid at the boundaries.

For the temporal discretization the ETD method is used. Due to the logarithmic transformation, the matrix of the coefficients is constant-valued, and thus, the matrix exponential is computed just once for all time levels.

For the approximation of the integral term in the case of the jump-diffusion models, the multivariate Gauss–Hermite quadrature has been implemented. The choice of this integration method is conditioned by the good approximation properties for low number of nodes (comparing to the trapezoidal and other Newton–Cotes formulas). Since the quadrature nodes do not necessary coincide with the spatial nodes of the domain, the multidimensional linear interpolation has been implemented, the algorithm has been described in detail.

The proposed GH-ETD method can be applied to European and American options due to the incorporation of the rationality function. In other words, setting the rationality parameter $\Lambda_{\text{Rat}} = 0$ corresponds to the European option, while $\Lambda_{\text{Rat}} \gg 0$ refers to American one.

Finally, we have considered many numerical examples to prove the versatility of the proposed GH-ETD method and to compare it with other known methods.

AUTHOR CONTRIBUTIONS

Rafael Company, Vera N. Egorova and Lucas Jodar contributed equally to this work. All authors have read and agreed to the published version of the manuscript.

ACKNOWLEDGEMENTS

This work has been partially supported by the Ministerio de Ciencia, Innovación y Universidades, Spanish grant MTM2017-89664-P and by the Spanish Ministry of Economy and Competitiveness MINECO through the project PID2019-107685RB-I00.

CONFLICT OF INTEREST STATEMENT

The authors declare no potential conflict of interests.

ORCID

Rafael Company https://orcid.org/0000-0001-5217-1889
Vera N. Egorova https://orcid.org/0000-0002-3024-3033
Lucas Jódar https://orcid.org/0000-0002-9672-6249

REFERENCES

1. F. Black and M. Scholes, *The pricing of options and corporate liabilities*, J. Political Econ. **81** (1973), no. 3, 637–654.
2. R. Cont and P. Tankov, *Financial modelling with jump processes*, Chapman & Hall/CRC Financial Mathematics Series (Boca Raton, Fla., London: Chapman & Hall/CRC), 2004.
3. L. Boen and K. Hout, *Operator splitting schemes for American options under the two-asset Merton jump-diffusion model*, Appl. Numer. Math. **153** (2020), 114–131. https://doi.org/10.1016/j.apnum.2020.02.004
4. R. Zvan, P. A. Forsyth, and K. R. Vetzal, *Penalty methods for American options with stochastic volatility*, J. Comput. Appl. Math. **91** (1998), no. 2, 199–218. https://doi.org/10.1016/s0377-0427(98)00037-5
5. A. Bensoussan and J. Lions, *Controle impulsionnel et inequations quasi variationnelles*, Vol. **11**, Gauthier-Villars, Paris, 1982.

10991476, 2023, 9, Downloaded from https://onlinelibrary.wiley.com/doi/10.1002/mma.9125 by Universidad De Cantabria, Wiley Online Library on [16/05/2023]. See the Terms and Conditions (https://onlinelibrary.wiley.com/terms-and-conditions) on Wiley Online Library for rules of use; OA articles are governed by the applicable Creative Commons License

6. D. Lamberton and B. Lapeyre, *Introduction to stochastic calculus applied to finance*, Chapman and Hall/CRC, New-York, 2007.
7. G. Wang, X. Wang, and K. Zhou, *Pricing vulnerable options with stochastic volatility*, Phys. A: Stat. Mech. Appl. **485** (2017), 91–103.
8. S. Wang, X. Q. Yang, and K. L. Teo, *Power penalty method for a linear complementarity problem arising from american option valuation*, J. Optim. Theory Appl. **129** (2006), no. 2, 227–254. https://doi.org/10.1007/s10957-006-9062-3
9. D. Lesmana and S. Wang, *Penalty approach to a nonlinear obstacle problem governing American put option valuation under transaction costs*, Appl. Math. Comput. **251** (2015), 318–330.
10. Y. D'Halluin, P. A. Forsyth, and G. Labahn, *A penalty method for American options with jump diffusion processes*, Numerische Mathematik **97** (2004), no. 2, 321–352. https://doi.org/10.1007/s00211-003-0511-8
11. J. Cruz and D. Ševčovič, *On solutions of a partial integro-differential equation in Bessel potential spaces with applications in option pricing models*, Japan J. Ind. Appl. Math. **37** (2020), no. 3, 697–721.
12. L. Andersen and J. Andreasen, *Jump-diffusion processes: volatility smile fitting and numerical methods for option pricing*, Rev. Derivatives Res. **4** (2000), no. 3, 231–262. https://doi.org/10.1023/A:1011354913068
13. R. Cont and E. Voltchkova, *A finite difference scheme for option pricing in jump diffusion and exponential lévy models*, SIAM J. Numer. Anal. **43** (2005), no. 4, 1596–1626. https://doi.org/10.1137/S0036142903436186
14. M. Fakharany, V. N. Egorova, and R. Company, *Numerical valuation of two-asset options under jump diffusion models using Gauss Hermite quadrature*, J. Comput. Appl. Math. **330** (2018), 822–834. https://doi.org/10.1016/j.cam.2017.03.032
15. D. Ahmadian, L. Ballestra, and N. Karimi, *An extremely efficient numerical method for pricing options in the Black Scholes model with jumps*, Math. Methods Appl. Sci. **44** (2021), no. 2, 1843–1862.
16. A. Ghosh and C. Mishra, *High-performance computation of pricing two-asset American options under the Merton jump-diffusion model on a GPU*, Comput. Math. Appl. **105** (2022), no. October 2021, 29–40. https://doi.org/10.1016/j.camwa.2021.11.012
17. D. Ahmadian and L. V. Ballestra, *A numerical method to price discrete double Barrier options under a constant elasticity of variance model with jump diffusion*, Int. J. Comput. Math. **92** (2015), no. 11, 2310–2328. https://doi.org/10.1080/00207160.2014.986114
18. L. Feng and V. Linetsky, *Pricing options in jump-diffusion models: an extrapolation approach*, Oper. Res. **56** (2007), no. 2, 304–325. https://doi.org/10.1287/opre.1070.0419
19. A. A. E. F. Saib, D. Y. Tangman, and M. Bhuruth, *A new radial basis functions method for pricing American options under Merton's jump-diffusion model*, Int. J. Comput. Math. **89** (2012), no. 9, 1164–1185.
20. M. Shirzadi, M. Dehghan, and A. Foroush Bastani, *On the pricing of multi-asset options under jump-diffusion processes using meshfree moving least-squares approximation*, 2020. Communications in Nonlinear Science and Numerical Simulation, 84.
21. R. Company, V. Egorova, L. Jódar, and F. Soleymani, *A mixed derivative terms removing method in multi-asset option pricing problems*, Appl. Math. Lett. **60** (2016), 108–114.
22. S. Clift and P. Forsyth, *Numerical solution of two asset jump diffusion models for option valuation*, Appl. Numer. Math. **58** (2008), no. 6, 743–782.
23. S. M. Cox and P. C. Matthews, *Exponential time differencing for stiff systems*, J. Comput. Phys. **176** (2002), no. 2, 430–455. https://doi.org/10.1006/jcph.2002.6995
24. R. Company, V. Egorova, L. Jódar, and F. Valls, *An ETD method for American options under the Heston model*, CMES - Comput. Model. Eng. Sci. **124** (2020), no. 2, 493–508.
25. C. R, E. V, and J. L, *A front-fixing etd numerical method for solving jump diffusion american option pricing problems*, Math. Comput. Simul. **189** (2021), 69–84.
26. N. Rambeerich, D. Y. Tangman, M. R. Lollchund, and M. Bhuruth, *High-order computational methods for option valuation under multifactor models*, Eur. J. Oper. Res. **224** (2013), no. 1, 219–226. https://doi.org/10.1016/j.ejor.2012.07.023
27. I. Karatzas and S. E. Shreve, *Methods of Mathematical Finance*, Applications of Mathematics: Stochastic Modelling and Applied Probability, Springer, 1998.
28. A. M. Poteshman and V. Serbin, *Clearly irrational financial market behavior: evidence from the early exercise of exchange traded stock options*, The J. Finance **58** (2003), no. 1, 37–70. https://doi.org/10.1111/1540-6261.00518
29. K. Gad and J. Pedersen, *Rationality parameter for exercising american put*, Risks **3** (2015), no. 2, 103–111.
30. R. Company, V. Egorova, L. Jódar, and C. Vázquez, *Finite difference methods for pricing American put option with rationality parameter: Numerical analysis and computing*, J. Comput. Appl. Math. **304** (2016), 1–17.
31. R. Company, V. Egorova, L. Jódar, and C. Vázquez, *Computing American option price under regime switching with rationality parameter*, Comput. Math. Appl. **72** (2016), no. 3, 741–754.
32. R. Company, V. N. Egorova, and L. Jódar, *Conditional full stability of positivity-preserving finite difference scheme for diffusion advection-reaction models*, J. Comput. Appl. Math. **341** (2018), 157–168.
33. P. J. Davis and P. Rabinowitz, *Methods of numerical integration, 2nd ed.,* W. Rheinbolt (eds.), Academic Press Inc., San Diego, California, 1984.
34. B. D. Keister, *Multidimensional quadrature algorithms*, Comput. Phys. **10** (1996), no. 2, 119–128. https://doi.org/10.1063/1.168565
35. H. J. Hogben, M. Krzystyniak, G. T. P. Charnock, P. J. Hore, and I. Kuprov, *Spinach A software library for simulation of spin dynamics in large spin systems*, J. Magn. Res. **208** (2011), no. 2, 179–194.
36. I. Kuprov, *Diagonalization-free implementation of spin relaxation theory for large spin systems*, J. Magn. Res. **209** (2011), no. 1, 31–38.

10991476, 2023, 9, Downloaded from https://onlinelibrary.wiley.com/doi/10.1002/mma.9125 by Universidad De Cantabria, Wiley Online Library on [16/05/2023]. See the Terms and Conditions (https://onlinelibrary.wiley.com/terms-and-conditions) on Wiley Online Library for rules of use; OA articles are governed by the applicable Creative Commons License

37. Y. D'Halluin, P. A. Forsyth, and K. R. Vetzal, *Robust numerical methods for contingent claims under jump diffusion processes*, IMA J. Numer. Anal. **25** (2005), no. 1, 87–112. https://doi.org/10.1093/imanum/drh011

How to cite this article: R. Company, V. N. Egorova, and L. Jódar, *An ETD method for multi-asset American option pricing under jump-diffusion model*, Math. Meth. Appl. Sci. 2023;46(9):10332–10347. doi.org/10.1002/mma.9125

10991476, 2023, 9, Downloaded from https://onlinelibrary.wiley.com/doi/10.1002/mma.9125 by Universidad De Cantabria, Wiley Online Library on [16/05/2023]. See the Terms and Conditions (https://onlinelibrary.wiley.com/terms-and-conditions) on Wiley Online Library for rules of use; OA articles are governed by the applicable Creative Commons License